Microchemical Journal 219 (2025) 115823

Contents lists available at ScienceDirect

Microchemical Journal

journal homepage: www.elsevier.com/locate/microc

A computer-based study on the potential flutamide drug biosensor based on transition metal modified BN nanocage

Osamah Abdulbari Khadhair [a], Ammar Yasir Ahmed [b,*], G. Padma Priya [c], Subhashree Ray [d], Amrita Pal [e], Vimal Arora [f], Otabek Mukhitdinov [g], Lola Safarova [h,i], Devendra Pratap Rao [j,**], Aseel Smerat [k,l], Safia Obaidur Rab [m]

[a] University of Warith Alanbiyaa, College of Engineering, Department of Biomedical Engineering, Iraq
[b] College of Pharmacy, University of Al Maarif, Al Anbar 31001, Iraq
[c] Department of Chemistry and Biochemistry, School of Sciences, JAIN (Deemed to be University), Bangalore, Karnataka, India
[d] Department of Biochemistry, IMS and SUM Hospital, Siksha 'O' Anusandhan (Deemed to be University), Bhubaneswar, Odisha 751003, India
[e] Department of chemistry Sathyabama Institute of Science and Technology, Chennai, Tamil Nadu, India
[f] University institute of Pharma Sciences, Chandigarh University, Mohali, Punjab, India
[g] Kimyo International University in Tashkent, Shota Rustaveli str. 156, Tashkent 100121, Uzbekistan
[h] New Uzbekistan University, Movarounnahr street 1, Tashkent 100000, Uzbekistan
[i] Samarkand State University of Veterinary Medicine, Livestock and Biotechnologies, Samarkand 140103, Uzbekistan
[j] Department of Chemistry, Coordination Chemistry Laboratory, Dayanand Anglo-Vedic (PG) College, Kanpur 208001, Uttar Pradesh, India
[k] Faculty of Educational Sciences, Al-Ahliyya Amman University, Amman 19328, Jordan
[l] Centre for Research Impact and Outcome, Chitkara University, Punjab, India
[m] Department of Clinical Laboratory Sciences, College of Applied Medical Sciences, King Khalid University, Abha, Saudi Arabia

ARTICLE INFO

Keywords:
Flutamide drug
BN-cage
Recovery time
Sensor
Electronic sensitivity

ABSTRACT

Recent studies have shown that BN-cage has the potential to act as a detector for various biological molecules such as drugs. Using density functional theory (DFT), this research investigated how sensitive pure and Ru metal-decorated BN-cage are to the anticancer drug flutamide (FLUT) at an electron level. In present work, calculations at the DFT-D3 level were conducted applying B3LYP functional and 6–31++G(d,p) basis set to explore energetic, geometric, and electronic characteristics of FLUT adsorption within pure BN nanocage and its modified forms. Findings indicated that FLUT undergoes physical adsorption within the BN cage with E_{ad} about −6.78 kcal/mol. In system with Ru metal decoration, FLUT interacts moderately with −38.55 kcal/mol energy and exhibits a satisfactory recovery time at ambient temperature ($\tau = 2.74 \times 10^{-2}$ s). The analysis of electronic sensitivity to FLUT adsorption revealed that Ru@BN-cage exhibited higher sensitivity (ΔE_{gap} = 89 %) than the pure cage. Furthermore, when investigating potential of a work function (Φ) sensor, Ru@BN-cage exhibited the most substantial response, with a 47.51 % alteration in system's Φ post gas adsorption. To sum up, due to observed alterations in work function and energy gap, it can be concluded that Ru@BN nanocage is stable and has the potential to serve as an electronic sensor material to specific detect of FLUT molecules in surrounding media.

1. Introduction

Cancer is a leading cause of death worldwide [1–3]. Some cancers can be cured if detected early and treated effectively [4–6]. A non-steroidal medication known as flutamide (FLUT) is chiefly used to treat prostate cancer, particularly in cases classified as locally advanced or metastatic. It is often administered alongside a class of drugs known as luteinizing hormone-releasing hormone (LHRH) agonists [7]. Moreover, ongoing work is investigating the potential uses of FLUT in treating a range of conditions and cancer types. Methods for detecting flutamide such as Soxhlet extraction system integrated with electrospray ionization (ESI) technique [8], spectrofluorimetric [9], and HPLC/UV [10]. Furthermore, FLUT can be identified and detected through a variety of electrochemical techniques [11]. These techniques rely on the

* Corresponding author.
** corresponding author.
E-mail addresses: ammar.yasir@uoa.edu.iq (A.Y. Ahmed), devendrapratapprao@yahoo.com (D.P. Rao).

https://doi.org/10.1016/j.microc.2025.115823
Received 1 September 2025; Received in revised form 25 September 2025; Accepted 17 October 2025
Available online 19 October 2025

utilization of diverse sensors and electrodes, like sensors based on graphene oxide (GO), screen-printed C electrodes, and diamond nanoparticles (SPCEs/DNPs) [12,13].Nowadays, different sensors have different applications in various areas [14–18]. Mentioned sensors demonstrated remarkable sensitivity with minimal detectable concentrations, outstanding selectivity and broad linear detection ranges for identifying FLUT concentrations. They were effectively employed in identifying flutamide in environmental samples like water bodies, as well as biological samples like urine, plasma, and serum [19,20]. In contrast to traditional analytical methods, thermal and electrochemical sensors offer superior advantages. Mentioned sensors are cost-effective, portable, compact devices that can operate autonomously. They provide essential instrumentation with outstanding sensitivity and selectivity, quick analysis times, and wide linear ranges. The crucial first step in developing a new sensor for analyte detection involves selecting a proper sensor material that interacts specifically with analyte of interest. Interaction has been anticipated to cause a significant change in sensor material's thermal or electrical conductance. The interaction of drugs with different surfaces is of great importance [21,22]. Various techniques like chronoamperometry, cyclic voltammetry (CV), and electrochemical impedance spectroscopy (EIS) have been typically utilized in this context. Investigations on FLUT has been widely investigated for its sensing potential through theoretical methodologies and Density functional theory (DFT) computations. Numerous investigations have concentrated on understanding the manner in which FLUT has interaction with various materials to advance biosensor technologies [23–26]. Through the utilization of advanced computational methods like DFT, researchers have successfully examined reactivity behavior and adsorption energy (E_{ads}) values of FLUT on metal-doped nanostructures, incorporating elements such as Zn, Ni, and Cu [27]. Study outcomes reveal that FLUT undergoes chemisorption on these nanostructures, exhibiting varying adsorption energies and degrees of reactivity. Additionally, researchers have scrutinized electronic properties such as molecular orbital interactions and band gaps to understand better sensing potential of these materials for FLUT. Mentioned works highlight significance of theoretical approaches and DFT computations in exploring sensing properties of FLUT and in the development of effective biosensors for detecting this anti-cancer medication. Currently, nanomaterials find widespread application across diverse scientific and industrial domains [28–30]. Distinct feature of various nanomaterial classes enables their wide-ranging uses [31–33]. The compatibility of nanomaterials with biological systems is crucial for effective utilization in biomedical fields like drug delivery and biosensing. Biosensors are analytical devices designed to identify and quantify a specific biological analyte [34,35]. Biosensors are essential in the development of advanced medical treatments and function as highly sensitive instruments for early disease detection [36–39]. Usually, a biosensor comprises three primary components: detector, transducer, and biological element. Biological element recognizes analyte, producing a response that the transducer translates into a measurable signal. This signal is then amplified, processed, and displayed on an electronic device [40].

Nanomaterials are increasingly gaining global significance due to their potential uses in different areas [41–45]. The include gas sensing applications [46,47], ion removal [48–50], medicine [51], food packing [52], and catalyst [53]. The advancement of boron nitrides, including nanotubes (BNNT), nanocages ($(BN)_n$), 2D nanotubes (h-BN), and nanoclusters (B_6N_6), for use as toxic gas sensors or in drug delivery has captured the attention of research teams in recent years. This interest is fueled by their potential for rapid detection, remarkable sensitivity, and minimal recovery time. Nevertheless, use of pristine $B_{12}N_{12}$ nanocages as sensors can be limited due to their relatively weak interactions with the BN nanocage surface [54–58]. Functionalizing nanostructures via transition metals (TMs) induces significant changes in their properties. Use of DFT has enabled the exploration of the role of first-row TMs in modifying nanostructures including nanotubes, nanocages, and macrocycles [59]. Density Functional Theory serves as a tool with significant computational capabilities, capable of simulating complex electronic structures and providing valuable insights in chemical research. For instance, it has been instrumental in studying acetone detection using WO_3, exploring gas adsorption on various $X_{12}Y_{12}$ nanocages systematically, and analyzing phosgene adsorption on copper-decorated BNNC [56,60,61]. DFT has further been utilized for impact simulation of electric fields on interactions with toxic gases, analyze macrocycles used in oxygen reduction reactions, and study detecting NO gas on copper-modified $B_{12}N_{12}$ structures [54,59]. These applications underscore the fundamental role that DFT has played in research and advancement of gas sensor technologies over time. Silva et al. [62] performed a comprehensive study of existing literature focusing on BN-cages in their pristine form and after modifications utilized in toxic gas detection, considering studies that employed DFT.

For FLUT sensing and adsorption, impact of modifications using transition metals on $B_{12}N_{12}$ nanocages (BN-cages) lacks coverage in scientific literature. Thus, objective of present work was to conduct a theoretical investigation using DFT to examine how decorations of BN-cage with transition metals (Ru) influence the interaction with FLUT and assess suitability of modified BN-cage as a sensing material for detecting FLUT drug in environmental settings.

2. Computational details

Gaussian 09 [63] has been applied for whole geometry optimization and energy computations. Whole computations have been carried out utilizing DFT approach at Lee-Yang-Parr exchange-correlation hybrid functional (B3LYP) [64–66], which is extensively employed in investigation of all-boron structures because of its widespread use in investigations [67,68]. A split valence double-ζ basis set 6–31++G(d,p) has been utilized along with corrected basis set superposition in computations [69]. After optimizing the structures at specified level, vibrational analysis has been conducted. Also, the LANL2DZ basis set method was used for the Ru metal. Presence of only positive vibrational frequencies verifies structural stability of optimized configurations. The SCF convergence thresholds were set tightly to ensure reliable results, with energy changes between iterations converged below 10^{-9} Hartree and density changes minimized appropriately. Integration grids were sufficiently dense to balance accuracy and efficiency, avoiding errors that could prevent SCF convergence. For spin states, especially concerning Ru, an appropriate spin multiplicity was assigned given its transition metal nature, accounting for potential open-shell configurations. These computational parameters were chosen to achieve stable and accurate modeling of the Ru@BN system. Natural bond orbital (NBO) approach was employed to analyze charge transfer interactions between BN-cage fullerenes and FLUT. Computation of HOMO-LUMO energy gap (E_g) was executed as follows:

$$E_g = E_{LUMO} - E_{HOMO} \tag{1}$$

Sensitivity of BN-cage towards FLUT was evaluated by analyzing change in HOMO-LUMO E_g as below [70,71]:

$$\Delta Eg = \frac{E_{g_2} - E_{g_1}}{E_{g_1}} \times 100\% \tag{2}$$

Herein, E_g values of pristine fullerenes and FLUT/BN-cage complexes are stated by E_{g1} and E_{g2}, respectively. Adsorption energy (E_{ads}) for interaction between FLUT drug and pure as well as decorated BN-cage was determined using the formula:

$$E_{ads} = E_{complex} - E_{BN-cage} - E_{drug} + E_{BSSE} \tag{3}$$

Computation included consideration of zero-point energy (ZPE). Based on Eq. (3), a negative E_{ads} signifies stability of FLUT/BN-cage complexes.

3. Results and discussion

3.1. FLUT adsorption over pristine BN-cage

Optimized structures, Molecular Electrostatic Potential (MEP) map, and highest Occupied molecular orbital of FLUT have been displayed in Fig. 1. Bond angles and distances are in good accordance with former computational and experimental studies [72,73]. As indicated by the MEP map, F and O atoms of the FLUT molecule displayed nucleophilic features owing to existence of lone electron pairs. These electron pairs are capable of effectively reacting with electron-deficient B atoms in BN-cage.

FLUT has been placed at various positions in the BN-cage, like top of heptagon or hexagon, with several B—N bonds connecting to its O, C, and F atoms, arranged in both horizontal and vertical orientations. After optimization, energetically most favorable configuration was achieved, as illustrated in Fig. 2. The results revealed that FLUT molecule binds to boron atoms of six-membered rings via its oxygen and fluorine atoms, exhibiting E_{ads} of −6.87 kcal/mol. Furthermore, thermodynamic parameters such as ΔH and ΔG suggested that FLUT molecule undergoes spontaneous and exothermic adsorption onto the pristine BN cage at room temperature, indicating favorable interaction under ambient conditions. In FLUT molecule, carbon–fluorine and nitrogen–oxygen bond lengths measure 1.30 Å and 1.19 Å, respectively. Moreover, O–N–O bond angle is 123.9°, while F–C–F angle is 34.8°. Post FLUT/BN complex forming, mentioned bond distances and angles remained relatively stable without significant changes. For FLUT, NBO charge in complex is 0.08 e, suggesting a transfer of charge from FLUT to BN-cage, with FLUT has electron donation role.

3.2. FLUT adsorption over Ru-decorated BN-cage

Former research has shown that ability of metal-decorated nanocages to adsorb molecules is substantially improved [74]. The design of metal-decorated BN-cages has attracted significant interest because of their versatility across different purposes. Hence, it is compelling to investigate influence of metal decoration on sensing capabilities of BN-cages. Consequently, effect of incorporating Ru with BN-cage over FLUT adsorption has been explored. Initially, Ru has been positioned above BN-cage without any symmetrical constraints. Following this, structure had optimization without restrictions. For Ru@BN-cage, multiplicity was chosen to be a doublet, and computations were performed using the unrestricted method. It was observed that the Ru metal tended for central area occupation. Analysis of geometrical configurations of Ru@BN-cage indicates that the Ru decoration of the BN-cage does not alter the cage structure. Following optimization, the Ru is situated at the central top of the BN-cage, ensuring that no deformation is induced in the BN-cage. To evaluate the stability of Ru on the BN-cage, the binding energy of the transition metal on the BN-cage was calculated. This binding energy was found to be greater than the cohesive energy of Ru in its metallic lattice, which demonstrates the strong stability of Ru adsorption on the BN-cage surface. This result indicates that Ru atoms are energetically favored to remain attached to the BN-cage rather than aggregating into bulk metal, confirming the robustness of the Ru@BN-cage system for potential applications.

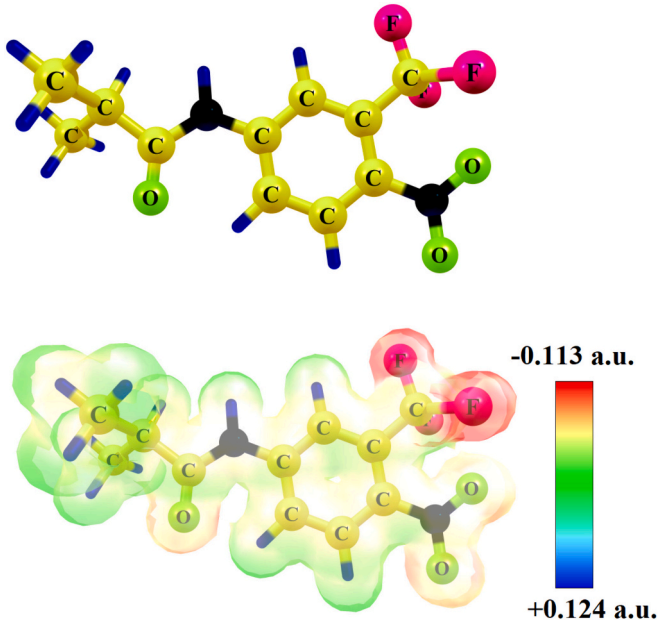

Fig. 1. The optimized structure and MEP map of FLUT molecule.

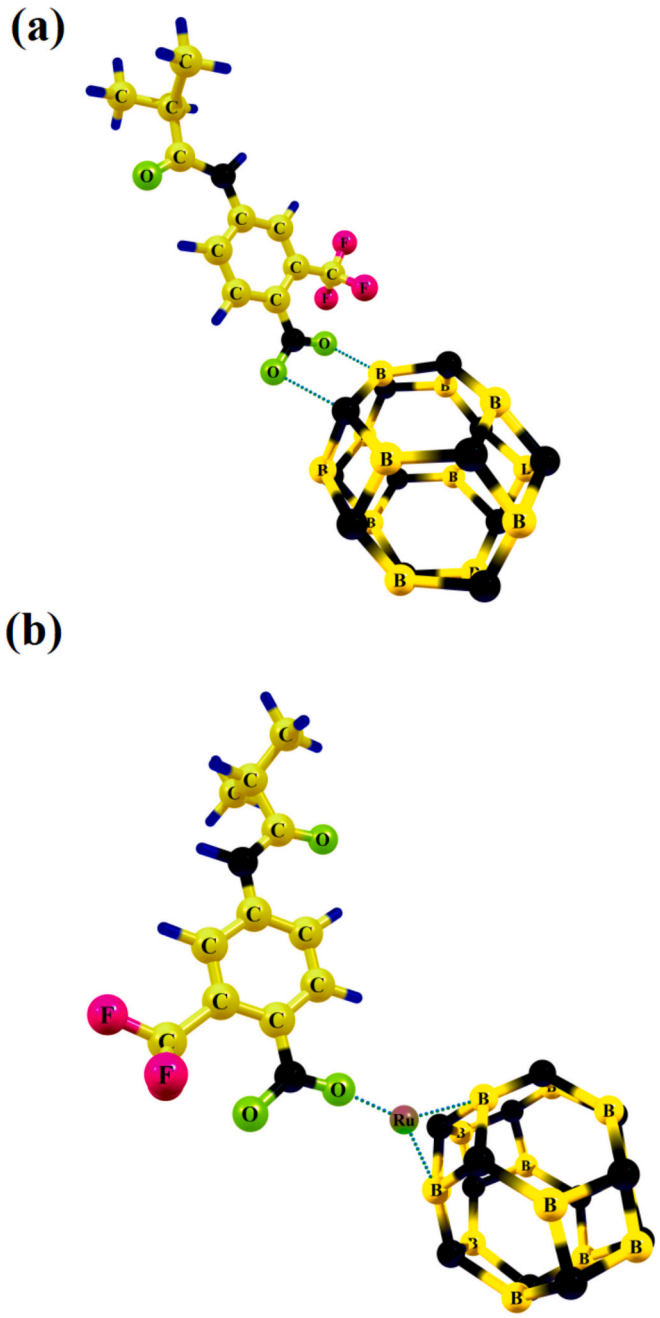

Fig. 2. The optimized structure of (a) pure and (b) Ru decorated BN nanocage complex with FLUT molecule.

Interaction of FLUT with Ru@BN-cage yields an interaction energy of approximately −38.55 kcal/mol, significantly higher than that of the pristine nanocage. This suggests that surface modification enhances the nanocage's affinity for FLUT. The intensified interaction is associated with more notable changes in the drug's bond lengths and bond angles, indicating structural modifications upon adsorption. Moreover, a significant NBO charge transfer of approximately 0.152 e takes place between the drug and the Ru@BN-cage, emphasizing substantial electronic interaction. Such surface decoration of nanomaterials is recognized for enhancing stability, targeting specificity, and drug adsorption by modifying physicochemical properties and encouraging stronger binding, as evidenced in recent research on nanoparticle functionalization for drug delivery. Results indicate that altering the surface of the nanocage effectively enhances both the strength and specificity of interactions between drugs and nanostructures, which is pivotal for improving drug delivery efficiency and therapeutic efficacy. Correlation between energy gap and electrical conductance is expressed as below [75]:

$$\sigma = AT^{3/2}\exp\left(\frac{-E_g}{2kT}\right) \quad (4)$$

Here, E_g denotes energy gap between HOMO and LUMO levels, T refers to absolute temperature, k stands for Boltzmann's constant, and σ represents electrical conductivity. Eq. (4) suggests that a decrease in E_g results in an improvement in σ value and an enhancement in reactivity. The band gap of Ru@BN-cage decreased from 2.83 eV to 1.50 eV after drug adsorption, indicating an effective interaction between the drug and the nanocage. In other words, the E_g of Ru@BN-cage decreased by 89 %, leading to increment in reactivity and σ value of these compounds compared to the pure BN-cage. Sensitivity of both BN-cage and Ru@BN-cage to FLUT drug was assessed using two parameters: E_g and work function (Φ). Previous research has indicated that E_g can be a reliable indicator of a nanostructure's responsiveness to different chemicals [76].

As per Eq. 4, a decrease in Eg results in a substantial rise in σ. Furthermore, influence of the FLUT over fullerenes and Fermi level has been studied, as these are pivotal aspects in Φ-type sensors, making use of a Kelvin oscillator device to evaluate alterations in Φ values before and after molecule adsorption [77]. Adsorption of a molecule onto the sensor leads to shifts in the Fermi level, which in turn modifies gate voltage and generating an electrical signal essential for detecting chemicals. Fermi level indicates energy needed electron removal from system.

$$\Phi = V_{el}(+\infty) - E_F \quad (5)$$

In this scenario, E_F stands for Fermi level energy, and V_{el} refers to electrostatic potential energy far from material's surface, typically assumed to be 0. As V_{el} approaches zero at an infinite distance, Φ is definable ad $\Phi = -E_F$. Fermi level energy is computed using the following formula:

$$E_F = E_{HOMO} + E_g/2 \quad (6)$$

Adjusting E_F could result in an alteration in amount of field emission detected in a sensor, as outlined by classical Richardson-Dushman Eq. [78]. Determination of alteration in Φ because of adsorption of FLUT is computed as below:

$$\Delta\Phi = \frac{\Phi_2 - \Phi_1}{\Phi_1} \times 100\% \quad (7)$$

Here, Φ_1 and Φ_2 correspond to work function values for the pristine BN-cage and the FLUT/BN-cage complex, respectively. According to data presented in Table 1, adsorption of FLUT molecule does not significantly alter the work function of the BN-cage. While, the value Φ of Ru@BN-cage after FLUT was changed significantly, thus the Ru@BN-cage is suggested as Φ type sensors.

Table 1
Adsorption energy (E_{ads}), HOMO-LUMO gas (E_g), change of E_g (%ΔE_g) and work function (Φ) and the change of Φ (%ΔΦ).

System	E_{ads} (kcal/mol)	E_g (eV)	%ΔE_g	Φ (eV)	%ΔΦ
BN-cage	–	5.86	–	−4.59	–
FLUT@BN	−6.78	4.92	−15.97	−4.41	−5.23
Ru@BN	–	2.83	–	−3.43	–
FLUT@RU-BN	−38.55	1.50	−89 %	−1.82	−47.51

E_g values for FLUT/BN-cage and FLUT/Ru@BN-cage are 4.92 eV and 1.50 eV, respectively, in gaseous medium. A decrease in E_g results in improvement in electrical conductance, as explained by eq. (4). Modifications in E_g values prior and subsequent to complex formation enhance sensitivity of decorated BN-cage compared to pristine BN-cage. This alteration can be translated into an electrical signal, aiding in adsorbate detection. Hence, it can be deduced that Ru@BN-cage shows potential as a viable option for detecting FLUT, particularly as an electronic sensor. Recent research has thoroughly investigated how metal doping influences material properties, involving a variety of metals, on optical and electrical characteristics of substrate materials. Investigations typically demonstrate that doping can substantially alter the structural, electrical, and optical properties [79,80]. Ru-decorated BN nanocage shows significantly better sensitivity and performance for drug detection compared to other transition metal-doped nanostructures. The presence of Ru enhances the interaction strength with the target molecule, leading to stronger adsorption, larger changes in electronic properties, and faster recovery times. These advantages make Ru@BN a promising and more efficient nanosensor material for detecting drugs like flutamide (see Table 2)

3.3. ELF and MEP analysis

ELF measurements indicate degree of electron localization, enabling differentiation between low and high levels of localization. Its high values suggest complete localization (covalent bonding), while low ELF values indicate weak charge density (non-covalent bonding). In case of isolated BN cage, results unveiled a consistent charge density distribution between nitrogen and boron atoms, with a higher density surrounding nitrogen atoms in comparison to boron atoms of nanocages. Nonetheless, upon inclusion of Ru metal within cage, a notable increase in electron density area has been observed around a boron atom of nanocage, obtaining a more negative charge. This phenomenon is visualized in ELF (Fig. 3b). The same boron atom serves as site for drug adsorption. ELF parameter indicates that, for boron nitride cage, A non-covalent interaction is present between the drug and the nanocage (c). Conversely, in case of drug adsorption over Ru@BN-cage, an electrostatic interaction akin to a poor polar covalent bond (d) is noted, as revealed by ELF values from 0.45 to 0.67. These findings align with the observed adsorption energy outcomes, validating the superior drug adsorption on the surface of Ru@BN-cage in comparison with pristine cage.

Table 2
Comparison of E_{ad}, variation of ΔE_g (%), variation %ΔΦ and recovery time for FLUT drug on the different nano material.

Material	E_{ad} (kcal/mol)	ΔE_g (%)	ΔΦ (%)	τ (s)	Ref
Ru@BN-cage	−38.55	−89.00	−47.51	2.74×10^{-2}	This work
ZnO nanosheet	−20.62	−91.12	25.89	1.97×10^{-3}	[81]
Na@B40-cage	−3.70	−3.00	−3.24	4.16×10^{-5}	[82]
graphdiyne	−18.31	−56.49	–	–	[83]
B_3O_3 nanosheet	−26.94	−37.10	–	–	[84]

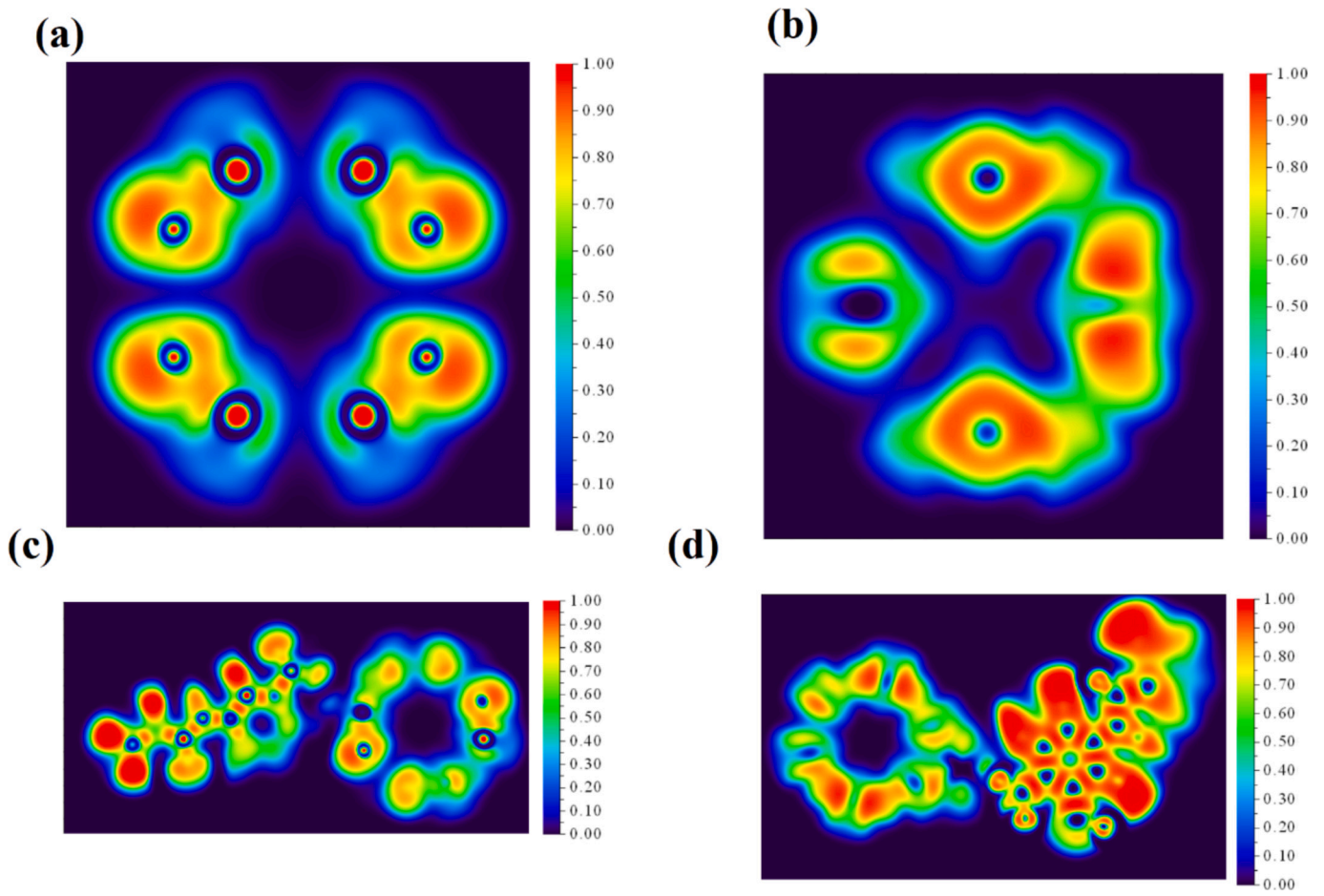

Fig. 3. The ELF graphs for the BN-cage and Ru@BN cage before and after adsorption of FLUT drug.

MEP illustrates electron density distribution across molecules, with regions of cationic environments (positive) displayed in blue hues, and areas of higher electronic charge density (negative) depicted in red. In Fig. 4, MEP of isolated BN cage (a) verifies that electron accumulation takes place around surrounding nitrogen, while the lowest electron density is observed surrounding boron atoms. As the FLUT molecule approaches, a positive region develops in BN (b), particularly on side where drug's oxygen atom comes close. In the Ru@BN-cage (c) system, a deviation into symmetrical charge distribution of nanocage has been noted, with emergence of an area exhibiting considerable electronic density over a boron atom, aligning with the observations in ELF. Moreover, the MEP of the FLUT/Ru@BN-cage system (d) illustrates a decrease in electron density within nanocage (blue) and a rise in electron density (red) over gas molecule. This observation supports and validates transfer of charges forecast from cage to gas as indicated by NBO data. Notably, MEP of FLUT/Ru@BN-cage system clearly demonstrates a more pronounced transfer of charges from cage to FLUT compared to other encapsulated configurations. This signifies presence of strong back-donation within system, accounting for cage's heightened sensitivity to gas. Consequently, MEP and ELF analyses confirm that doping BN cage with Ru yields a nanocage that, in comparison to the FLUT molecule, exhibits enhanced sensitivity, improved thermodynamic stability, moderate physisorption, increased charge transfer, and strong potential for sensor applications.

3.4. Recovery time (τ)

Significant interactions are vital in the advancement of electronic sensors, rendering the desorption process complex. Even in absence of theoretical backing, evaluating response time proves to be difficult. Nonetheless, τ can be assessed utilizing transition state theory. As per Eq. (8), enhancing E_{ads} will lead to a prolonged τ for interaction [85]:

$$\tau = \frac{1}{\upsilon}\exp\left(\frac{-E_{ads}}{kT}\right) \quad (8)$$

Herein, k presents Boltzmann constant, υ is attempt frequency to 10^{12} Hz, and ambient temperature (298.15 K) has been indicated by T. E_{ads} is exponentially related τ. Value of τ for BN-cage and Ru@BN-cage are 1.89×10^{-6} and 2.74×10^{-2} s respectively. These findings indicate that both BN have small τ value, and FLUT is reversibly adsorbed. Results suggest that τ of Pramipexole molecules from Au surfaces at 298 K is similar, spanning from 1.2 milliseconds to around 105 s [86]. In a distinct study, τ for adrucil/Al-doped phagraphene (ADP) complex has been determined to be approximately 4.09×10^{18} s at similar temperature [87]. This implies that ADP demonstrates an extraordinarily extended τ, making it ineffective for use as a drug carrier.

Ru@BN nanocage offers enhanced FLUT detection compared to previously studied metal-doped BN nanostructures by showing stronger adsorption energy, higher electronic sensitivity (89 % change in energy gap), a more significant work function response (47.51 % change), and faster recovery time. These improvements highlight the unique advantage of Ru decoration in increasing selectivity and sensing efficiency, setting Ru@BN apart as a novel, more effective sensor material for FLUT detection.

3.5. Solvent effect

The influence of H_2O solvent on the adsorption of the FLUT drug on

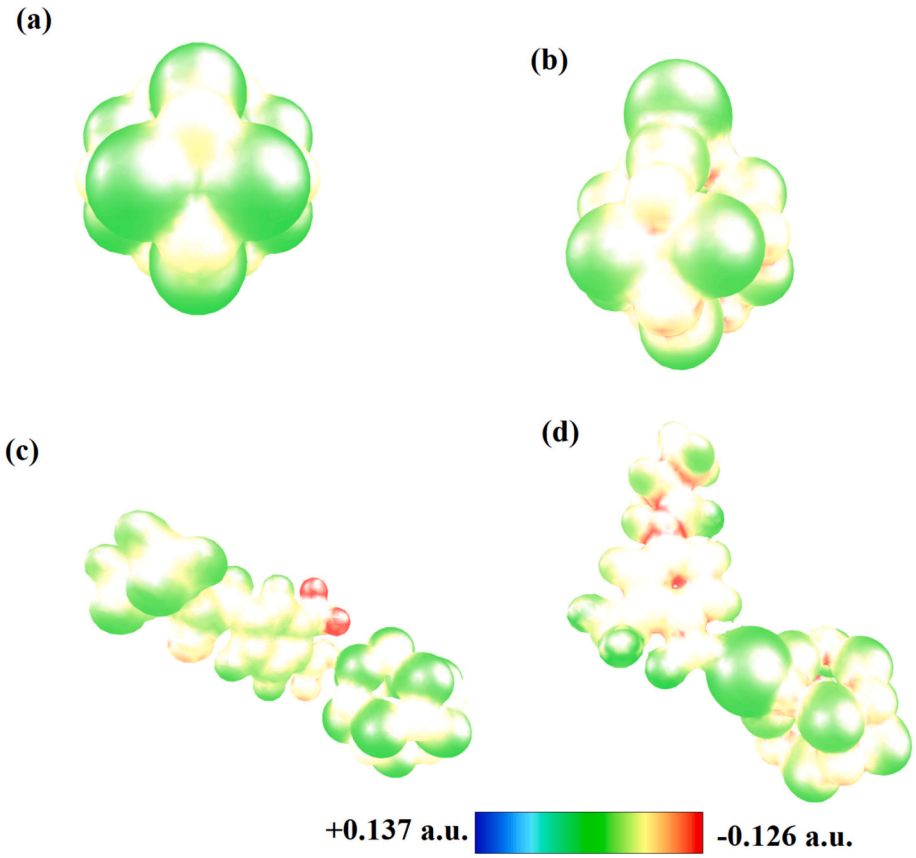

Fig. 4. Molecular electrostatic potential (MEP) map for the BN-cage and Ru@BN cage before and after adsorption of FLUT drug.

the Ru@BN-cage was considered using the Polarizable Continuum Model (PCM) method. The FLUT drug, Ru@BN-cage, and their complex were re-optimized in water. The calculations revealed that the interaction between FLUT and Ru@BN-cage slightly weakened in the solvent environment, with the adsorption energy (E_{ad}) decreasing to −27.88 kJ/mol. This approach ensures more realistic modeling of practical aqueous sensing conditions while maintaining computational efficiency. The influence of H_2O solvent on the adsorption of the FLUT drug on the Ru@BN-cage was considered by means of the PCM method. We once more optimized the FLUT drug, Ru@BN-cage, and complex with drug in the water. The calculations show that the interaction between FLUT drug and Ru@BN-cage slightly weakened and the E_{ad} decreased to −7.62 kcal/mol. However, one can write:

$$\Delta E_{ad\text{-}sol\text{-}gas} = E_{ad\text{-}solution}\text{-}E_{ad\text{-}gas} = 3.32\ \text{kcal/mol} \quad (9)$$

where $\Delta E_{ad\text{-}sol\text{-}gas}$ is the difference between the $E_{ad\text{-}solution}$ of FLUT in the gas phase and H_2O solvent. To further scrutinize this issue, the solvation energies ($\Delta E_{solution}$) of the FLUT, Ru@BN-cage, and FLUT/Ru@BN-cage were computed using the next equation:

$$\Delta E_{solution} = E_{solution}\text{-}E_{gas} \quad (10)$$

where $E_{solution}$ or E_{gas} is the energy of a system in the H_2O solvent or gas. The calculated solvation energies ($\Delta_{Esolution}$) for the FLUT drug, Ru@BN-cage, and the FLUT/Ru@BN-cage complex are −5.63, −7.29, and −15.98 kcal/mol, respectively. These results indicate that the solvation energy of the FLUT/Ru@BN-cage complex is less negative than the sum of the solvation energies of the individual FLUT drug and Ru@BN-cage components. This suggests that both the FLUT drug and Ru@BN-cage are highly polar systems with strong solubility in water. Consequently, water molecules tend to surround the FLUT drug and the Ru@BN-cage, which partially hinders their direct interaction.

4. Conclusion

Through DFT computations, we investigated FLUT adsorption over surfaces of both pristine and Ru-decorated BN-cage to develop an electronic sensor to detect FLUT anticancer medication. Findings indicated that the interaction between Ru@BN-cage and drug has been slightly stronger compared to the interaction between FLUT and the unmodified BN-cage. The thermodynamic analysis of the FLUT adsorption process revealed physical adsorption, identified as spontaneous and exothermic at ambient temperature. Remarkably, drug adsorption resulted in a reduction in Eg of BN-cage. Eg decline serves to boost electrical conductance of BN-cage, consequently producing an electrical signal. The produced signal serves as a dependable indicator of the FLUT anticancer medication's attendance, indicating that both the pristine and Ru-decorated forms of the BN-cage have potential as electronic sensors to detect FLUT. Investigation also disclosed that Φ of pristine BN-cage remains unaltered after the adsorption of FLUT molecules, whereas the Ru decoration of the BN-cage experiences a notable shift in the work function. As a result, the work function of the Ru-decorated configuration is suggested for deployment as Φ-type sensors. The only exception is the FLUT/Ru@BN-cage system, exhibiting moderate physisorption (with $E_{ads} = -38.55$ kcal/mol) and a rapid recovery time at ambient temperature ($\tau = 2.74 \times 10^{-2}$ s). MEP and ELF outcomes validate the observed shifts in Eg following adsorption, emphasizing poor interaction between medication and unaltered BN-cage, as well as covalent characteristic of interaction between Ru@BN-cage and drug. These features underscore FLUT/Ru@BN-cage system as a highly prospective contender for utilization in sensors designed for FLUT drug detection.

CRediT authorship contribution statement

Osamah Abdulbari Khadhair: Writing – original draft, Visualization, Software, Resources, Investigation. **Ammar Yasir Ahmed:** Writing – review & editing, Project administration, Methodology, Investigation, Data curation, Conceptualization. **G. Padma Priya:** Writing – original draft, Visualization, Resources, Methodology. **Subhashree Ray:** Software, Resources, Methodology, Investigation. **Amrita Pal:** Writing – original draft, Visualization, Methodology, Investigation. **Vimal Arora:** Visualization, Software, Resources, Conceptualization. **Otabek Mukhitdinov:** Writing – original draft, Visualization, Methodology, Investigation, Formal analysis. **Lola Safarova:** Software, Resources, Methodology, Investigation. **Devendra Pratap Rao:** Methodology, Investigation, Formal analysis, Conceptualization. **Aseel Smerat:** Methodology, Investigation, Formal analysis, Data curation, Conceptualization. **Safia Obaidur Rab:** Software, Funding acquisition, Formal analysis, Conceptualization.

Ethical approval

Not required.

Funding

None.

Declaration of competing interest

The authors declare that they have no known competing financial interests or personal relationships that could have appeared to influence the work reported in this paper.

Acknowledgments

The authors are thankful to the Deanship of Research and Graduate Studies, King Khalid University, Abha, Saudi Arabia, for financially supporting this work through the Large Research Group Project under Grant no. R.G.P.2/480/46.

Data availability

Data will be made available on request.

References

[1] C.-Y. Hsu, O.Q.B. Allela, S.A.-H. Mahdi, O.P. Doshi, M. Adil, M.S. Ali, M.J. Saadh, Pathology Res. Pract. 250 (2023) 154794.
[2] C.Y. Hsu, A. Faisal, S.S. Jumaa, N.S. Gilmanova, M. Ubaid, A.H. Athab, R. Mirzaei, S. Karampoor, Non-coding RNA Res 9 (2024) 970–994.
[3] C.Y. Hsu, H. Pallathadka, J. Gupta, H. Ma, H.H. Al-Shukri, A. Kareem, A. H. Zwamel, Y.F. Mustafa, Phytother Res 38 (2024) 4336–4350.
[4] C.-Y. Hsu, H. Pallathadka, S.A. Jasim, J. Rizaev, D. Olegovich Bokov, A. Hjazi, S. Mahajan, Y.F. Mustafa, B. Husseen, M.A. Jawad, Crit. Rev. Oncol. Hematol. 206 (2025) 104588.
[5] C.-Y. Hsu, A.T. Ahmed, S.O. Rab, S. Uthirapathy, S. Ballal, R. Kalia, R. Arya, D. Nathiya, M. kariem, A.J. Kadhim, Exp. Cell Res. 445 (2025) 114424.
[6] C.Y. Hsu, F.M. Altalbawy, E.F. Oghenemaro, S. Uthirapathy, M. Chandra, D. Nathiya, P. Kaur, M. Ravi Kumar, A.J. Kadhim, M. Kariem, Arch. Pharmazie 358 (2025) e202400940.
[7] A.V. Marenich, C.J. Cramer, D.G. Truhlar, C.A. Guido, B. Mennucci, G. Scalmani, M.J. Frisch, Practical computation of electronic excitation in solution: vertical excitation model, Chem. Sci. 2 (2011) 2143–2161.
[8] N. Khan, H.N. Abdelhamid, J.-Y. Yan, F.-T. Chung, H.-F. Wu, Detection of flutamide in pharmaceutical dosage using higher electrospray ionization mass spectrometry (ESI-MS) tandem mass coupled with Soxhlet apparatus, Analytical Chemistry Research 3 (2015) 89–97.
[9] A.A. Smith, R. Manavalan, K. Kannan, N. Rajendiran, Spectrofluorimetric determination of flutamide in pharmaceutical preaparations, Orient. J. Chem. 24 (2008) 189.
[10] S. Esmaeilzadeh, H. Valizadeh, P. Zakeri-Milani, A simple, fast, low cost, HPLC/UV validated method for determination of flutamide: application to protein binding studies, Advanced Pharmaceutical Bulletin 6 (2016) 251.
[11] T. Kokulnathan, R. Vishnuraj, T.-J. Wang, E.A. Kumar, B. Pullithadathil, Heterostructured bismuth oxide/hexagonal-boron nitride nanocomposite: a disposable electrochemical sensor for detection of flutamide, Ecotoxicol. Environ. Saf. 207 (2021) 111276.
[12] R. Karthik, M. Govindasamy, S.-M. Chen, T.-W. Chen, A. Elangovan, V. Muthuraj, M.-C. Yu, A facile graphene oxide based sensor for electrochemical detection of prostate anti-cancer (anti-testosterone) drug flutamide in biological samples, RSC Adv. 7 (2017) 25702–25709.
[13] P.K. Brahman, L. Suresh, K.R. Reddy, B. Js, An electrochemical sensing platform for trace recognition and detection of an anti-prostate cancer drug flutamide in biological samples, RSC Adv. 7 (2017) 37898–37907.
[14] Q. He, H. Luo, L. Chen, J. Dong, K. Chen, Y. Ning, Nanographite-based fluorescent ⁋biosensor for detecting microRNA using duplex-specific nuclease-assisted recycling, ⁋Luminescence 35 (3) (2020) 347–354, https://doi.org/10.1002/bio.3733⁋.
[15] T. Li, L. Xiao, H. Ling, Y. Yang, S. Zhong, Preparation of artificial substrate ⁋binding sites of nanozyme with "modular structure" strategy used for the construction of visual ⁋sensing analysis platform for levodopa, Microchemical Journal 212 (2025) 113292, https://doi.org/10.1016/j.microc.2025.113292⁋.
[16] T. Xianfang, L. Cai, Y. Meng, J. Xu, C. Lu, J. Yang, Indicator Regularized Non-Negative Matrix Factorization Method-Based Drug Repurposing for COVID-19, Frontiers in Immunology 11 (2021), https://doi.org/10.3389/fimmu.2020.603615.
[17] J. Wu, X. Yue, T. Wang, Y. Zhang, Y. Jin, G. Li, A cost-effective and sensitive ⁋voltammetric sensor for determination of baicalein in herbal medicine based on shuttle-shape ⁋α-Fe2O3 nanoparticle decorated multi-walled carbon nanotubes, Colloids and Surfaces A: ⁋Physicochemical and Engineering Aspects 717 (2025) 136850, https://doi.org/10.1016/j.colsurfa.2025.136850⁋.
[18] J. Yi, W. Xiao, G. Li, P. Wu, Y. He, C. Chen, T. Kai, The research of aptamer ⁋biosensor technologies for detection of microorganism, Applied Microbiology and ⁋Biotechnology 104 (23) (2020) 9877–9890, https://doi.org/10.1007/s00253-020-10940-1⁋.
[19] H. Wang, J.T. Robinson, G. Diankov, H. Dai, Nanocrystal growth on graphene with various degrees of oxidation, J. Am. Chem. Soc. 132 (2010) 3270–3271.
[20] R. Karthik, N. Karikalan, S.-M. Chen, P. Gnanaprakasam, C. Karuppiah, Voltammetric determination of the anti-cancer drug nilutamide using a screen-printed carbon electrode modified with a composite prepared from β-cyclodextrin, gold nanoparticles and graphene oxide, Microchim. Acta 184 (2017) 507–514.
[21] S. Wang, C. Yang, L. Chen, LSA-DDI: Learning Stereochemistry-Aware Drug ⁋Interactions via 3D Feature Fusion and Contrastive Cross-Attention, International Journal of ⁋Molecular Sciences 26 (14) (2025) 6799, https://doi.org/10.3390/ijms26146799⁋.
[22] K. Dou, W. Zhao, C. Wang, Y. Fan, C. He, L. Zhang, S. Pang, Switch on amine ⁋substrate reactivity towards hexaazaisowurtzitane cage: Insights from a tailored machine ⁋learning model, Chemical Engineering Journal 501 (2024) 157677, https://doi.org/10.1016/j.cej.2024.157677⁋.
[23] B. Agrahari, S. Layek, R. Ganguly, N. Dege, D.D. Pathak, Synthesis, characterization and single crystal X-ray studies of pincer type Ni (II)-Schiff base complexes: application in synthesis of 2-substituted benzimidazoles, J. Organomet. Chem. 890 (2019) 13–20.
[24] M. Kamel, K. Mohammadifard, Thermodynamic and reactivity descriptors studies on the interaction of Flutamide anticancer drug with nucleobases: a computational view, Chemical Review and Letters 4 (2021) 54–65.
[25] M. El-Mansy, O. Osman, A.A. Mahmoud, H. Elhaes, A. Gawad, M.A. Ibrahim, Computational notes on the chemical stability of flutamide, Lett. Appl. NanoBioScience 9 (2020) 1147–1155.
[26] J.B. Pandya, S.M. Shinde, P.K. Jha, Theoretical study on the interaction of flutamide anticancer drug with cucurbit [n] uril (n= 5–8) as a drug delivery system, Int. J. Quantum Chem. 122 (2022) e26899.
[27] E.U. Ejiofor, J.E. Ishebe, I. Benjamin, G.A. Okon, T.E. Gber, H. Louis, Exploring the potential of single-metals (cu, Ni, Zn) decorated Al12N12 nanostructures as sensors for flutamide anticancer drug, Heliyon 9 (2023).
[28] M.A. Raza, U. Farwa, M. Danish, S. Ozturk, A.A. Aagar, N. Dege, S.U. Rehman, A. G. Al-Sehemi, Computational modeling of imines based anti-oxidant and anti-esterases compounds: synthesis, single crystal and in-vitro assessment, Comput. Biol. Chem. 104 (2023) 107880.
[29] M.R. Jedla, B. Koneru, A. Franco, D. Rangappa, P. Banerjee, Recent developments in nanomaterials based adsorbents for water purification techniques, Biointerface Res. Appl. Chem 12 (2022) 5821–5835.
[30] E. Alphandéry, Ultrasound and nanomaterial: an efficient pair to fight cancer, J. Nanobiotechnol. 20 (2022) 139.
[31] H. Rahman, M.R. Hossain, T. Ferdous, The recent advancement of low-dimensional nanostructured materials for drug delivery and drug sensing application: a brief review, J. Mol. Liq. 320 (2020) 114427.
[32] F. Yuan, Y. Xia, Q. Lu, Q. Xu, Y. Shu, X. Hu, Recent advances in inorganic functional nanomaterials based flexible electrochemical sensors, Talanta 244 (2022) 123419.
[33] Y. Deng, Z. Sun, L. Wang, M. Wang, J. Yang, G. Li, Biosensor-based assay of exosome biomarker for early diagnosis of cancer, Frontiers of medicine (2022) 1–19.
[34] K. Dyussembayev, P. Sambasivam, I. Bar, J.C. Brownlie, M.J. Shiddiky, R. Ford, Biosensor technologies for early detection and quantification of plant pathogens, Front. Chem. 9 (2021) 636245.
[35] X. Zhu, H. Chen, Y. Zhou, J. Wu, S. Ramakrishna, X. Peng, H.S. Nanda, Y. Zhou, Recent advances in biosensors for detection of exosomes, Current Opinion in Biomedical Engineering 18 (2021) 100280.

[36] S. Chupradit, S.A. Jasim, D. Bokov, M.Z. Mahmoud, A.B. Roomi, K. Hachem, M. Rudiansyah, W. Suksatan, R. Bidares, Recent advances in biosensor devices for HER-2 cancer biomarker detection, Anal. Methods 14 (2022) 1301–1310.
[37] E. Egamberdiev, N. Shavazi, M.J. Kadham, S. Kasimova, N. Mamatmusayeva, D. Nabieva, G. Avezova, M. Bekchanova, S. Chuponov, N. Rustamova, F. Oripova, N. Dustova, G. Ikhtiyarova, Advances in electrochemical biosensors for early detection of rheumatoid arthritis, Clinica Chimica Acta 578 (2026) 120547.
[38] E. Egamberdiev, N. Shavazi, M.J. Kadham, S. Kasimova, N. Mamatmusayeva, D. Nabieva, G. Avezova, M. Bekchanova, S. Chuponov, N. Rustamova, F. Oripova, N. Dustova, G. Ikhtiyarova, Advances in electrochemical biosensors for early detection of rheumatoid arthritis, Clinica Chimica Acta 578 (2026) 120547.
[39] W. Al-Mussawi, A.Y. Ahmed, N.S. Sawaran Singh, S. Ganesan, B. Samantaray, M. Latipova, Y. Yusupov, R. Siddikov, A. Smerat, W.A. Yousif, M. Abohassan, Selective detection of gamma-butyrolactone drug using hexa-peri-hexabenzocoronene nanographene functionalized with amidoamine groups, Journal of Physics and Chemistry of Solids 209 (2026) 113277.
[40] M. Shobana, Nanoferrites in biosensors–a review, Mater. Sci. Eng. B 272 (2021) 115344.
[41] H. Wang, C. Tang, Y. Xiang, C. Zou, J. Hu, G. Yang, W. Zhou, Tea polyphenol-derived nanomedicine for targeted photothermal thrombolysis and inflammation suppression, Journal of Nanobiotechnology 22 (1) (2024) 146, https://doi.org/10.1186/s12951-024-02446-z.
[42] Q. Fang, Q. Sun, J. Ge, H. Wang, J. Qi, Multidimensional engineering of nanoconfined cCatalysis: frontiers in carbon-based energy conversion and utilization, Catalysts 15 (2025) 477.
[43] K. Xu, C. Liu, K. Kang, Z. Zheng, S. Wang, Z. Tang, W. Yang, Isolation of nanocrystalline cellulose from rice straw and preparation of its biocomposites with chitosan: Physicochemical characterization and evaluation of interfacial compatibility, Composites Science and Technology 154 (2018) 8–17.
[44] Yu Chen, Yuting Zhang, Juan Long, Xu Kaimeng, Tuhua Zhong, Multiscale cellulose-based optical management films with tunable transparency and haze fabricated by different bamboo components and mechanical defibrillation approaches, Carbohydrate Polymers 348 (2025) 122811.
[45] Yuting Zhang, Yu. Qiushi Li, Yizhong Cao Chen, Juan Wang, Jing Yang, Linkun Xie, Xijuan Chai, Lianpeng Zhang, Siqun Wang, Guanben Du, Kaimeng Xu, Effects of facile chemical pretreatments on physical-chemical properties of large clustered and small monopodial bamboo microfibers isolated by steam explosion, Industrial Crops & Products 207 (2024) 117747.
[46] G. Su, J. Xiong, Q. Li, S. Luo, Y. Zhang, T. Zhong, D.P. Harper, Z. Tang, L. Xie, X. Chai, Gaseous formaldehyde adsorption by eco-friendly, porous bamboo carbon microfibers obtained by steam explosion, carbonization, and plasma activation, Chemical Engineering Journal 455 (2023) 140686.
[47] J. Xiong, Y. Wang, H. Wang, L. Xie, X. Chai, L. Zhang, W. Peng, S. Wang, G. Du, K. Xu, Electrospun biomass carbon-based porous nanofibers modified by green-dry cold plasma for gaseous formaldehyde adsorption, Industrial Crops and Products 222 (2024) 119769.
[48] K. Zhang, C. Zhu, L. Xie, L. Zhang, X. Chai, C. Wu, S. Wang, W. Peng, G. Du, K. Xu, Facile fabrication of electrospun hybrid nanofibers integrated cellulose, chitosan with ZIF-8 for efficient remediation of copper ions, Carbohydrate Polymers 359 (2025) 123574.
[49] R. Luo, K. Zhang, Y. Qin, L. Xie, X. Chai, L. Zhang, G. Du, S. Ge, M. Rezakazemi, T. M. Aminabhavi, Amine-functionalized UiO-66 incorporated electrospun cellulose/chitosan porous nanofibrous membranes for removing copper ions, Chemical Engineering Journal 480 (2024) 148077.
[50] J. Xiong, Q. Hu, J. Wu, Z. Jia, S. Ge, Y. Cao, J. Zhou, Y. Wang, J. Yan, L. Xie, Structurally stable electrospun nanofibrous cellulose acetate/chitosan biocomposite membranes for the removal of chromium ions from the polluted water, Advanced Composites and Hybrid Materials 6 (2023) 99.
[51] M. Zhang, J. Zhou, X. Jiang, T. Shi, X. Jin, Y. Ren, K. Ji, Z. Xin, Z. Zhang, C. Yin, MoS2 Nanozyme–Chlorella Hydrogels: Pioneering a Hepatocellular Carcinoma Integrative Therapy, Advanced Functional Materials 35 (2025) 2417125.
[52] K. Xu, Q. Li, L. Xie, Z. Shi, G. Su, D. Harper, Z. Tang, J. Zhou, G. Du, S. Wang, Novel flexible, strong, thermal-stable, and high-barrier switchgrass-based lignin-containing cellulose nanofibrils/chitosan biocomposites for food packaging, Industrial Crops and Products 179 (2022) 114661.
[53] K. Yang, C. Li, Q. Zhu, H. Wang, J. Qi, Rich Oxygen Vacancies in Bimetallic MnCo2O4. 5 Spheres for Enhancing Lean Methane Catalytic Oxidation, Nanomaterials 15 (2025) 524.
[54] N. de Sousa Sousa, A.L.P. Silva, A.C.A. Silva, J. de Jesus Gomes, Varela Júnior, Cu-modified B12N12 nanocage as a chemical sensor for nitrogen monoxide gas: a density functional theory study, J. Nanopart. Res. 25 (2023) 248.
[55] A.L.P. Silva, J. de Jesus Gomes, Varela Júnior, Carbon monoxide interaction with B12N12 nanocage with and without an external electric field: a DFT study, J. Nanopart. Res. 24 (2022) 1.
[56] S. Hussain, R. Hussain, M.Y. Mehboob, S.A.S. Chatha, A.I. Hussain, A. Umar, M. U. Khan, M. Ahmed, M. Adnan, K. Ayub, Adsorption of phosgene gas on pristine and copper-decorated B12N12 nanocages: a comparative DFT study, ACS Omega 5 (2020) 7641–7650.
[57] M.J. Saadh, A. Basem, Z.A. Hanoon, M. Al-Bahrani, J. Mgm, J.C. Jie, K. Muzammil, M.A. Hasan, S. Islam, R. Zainul, Adsorption of NH3, HCHO, SO2, and Cl2 gasses on the o-B2N2 monolayer for its potential application as a sensor, Diamond Relat. Mater. 147 (2024).
[58] M.A. Yeamin, A. Hosen, M.A. Hossain, H.A. Abdulhussein, R.K. Pingak, S. Joifullah, W.H. Hassan, M.S. Abu-Jafar, T.A. Geleta, Study on pressure-induced band gap modulation and physical properties of direct band gap Ca3NX3 (X = cl, Br) for optoelectronic and thermoelectric applications, Surf Interfaces 56 (2025).
[59] N. de Sousa Sousa, R.B. de Lima, A.L.P. Silva, A.A. Tanaka, A.B.F. da Silva, J.D.J.G. V. Júnior, Theoretical study of dibenzotetraaza [14] annulene complexes with first row transition metals, Computational and Theoretical Chemistry 1054 (2015) 93–99.
[60] P. Wang, S. Guo, Y. Zhao, Z. Hu, Y. Tang, L. Zhou, T. Li, H.-Y. Li, H. Liu, WO3 nanoparticles supported by Nb2CTx MXene for superior acetone detection under high humidity, Sens. Actuators B 398 (2024) 134710.
[61] M.J. Saadh, A.B.M. Ali, Z. Hanoon, V. Jain, P.K. Pathak, A. Kumar, A.A. Almehizia, D.P. Rao, The ability of ZnO and MgO nanocages for adsorption and sensing performance of anticancer drug detection, J. Mol. Graph. Model. 137 (2025).
[62] A.L.P. Silva, N. de Sousa Sousa, J. de Jesus Gomes, Varela Júnior, Theoretical studies with B12N12 as a toxic gas sensor: a review, J. Nanopart. Res. 25 (2023) 22.
[63] M. Frisch, gaussian 09, Revision d. 01, Gaussian, Inc, Wallingford CT, 201, 2009.
[64] A.D. Becke, Density-functional exchange-energy approximation with correct asymptotic behavior, Phys. Rev. A 38 (1988) 3098.
[65] Y. Zhao, D.G. Truhlar, Density functionals with broad applicability in chemistry, Acc. Chem. Res. 41 (2008) 157–167.
[66] R. Zainul, A. Basem, A.K. Nemah, R. Kumar, R. Kumar, R. Sharma, A.M. Aljeboree, M. Chahar, Y. Elmasry, BP-biphenylene monolayers: a promising anode material for high-performance magnesium-ion batteries, Inorg. Chem. Commun. 168 (2024).
[67] T.R. Galeev, Q. Chen, J.-C. Guo, H. Bai, C.-Q. Miao, H.-G. Lu, A.P. Sergeeva, S.-D. Li, A.I. Boldyrev, Deciphering the mystery of hexagon holes in an all-boron graphene α-sheet, Phys. Chem. Chem. Phys. 13 (2011) 11575–11578.
[68] A.P. Sergeeva, Z.A. Piazza, C. Romanescu, W.-L. Li, A.I. Boldyrev, L.-S. Wang, B22–and B23–: all-boron analogues of anthracene and phenanthrene, J. Am. Chem. Soc. 134 (2012) 18065–18073.
[69] H. Kruse, L. Goerigk, S. Grimme, Why the standard B3LYP/6-31G* model chemistry should not be used in DFT calculations of molecular thermochemistry: understanding and correcting the problem, J. Org. Chem. 77 (2012) 10824–10834.
[70] N.M. O'boyle, A.L. Tenderholt, K.M. Langner, Cclib: a library for package-independent computational chemistry algorithms, J. Comput. Chem. 29 (2008) 839–845.
[71] M.J. Saadh, A.B.M. Ali, H.A. Kenjrawy, P. Sharma, A. Ismael Saber, G.V. Siva Prasad, A.R. Tameemi, A. Elawady, S. Qamar, S. Islam, Analysis of electronic properties and sensing applications in graphene/BC3 heterostructures, J Photochem Photobiol A Chem 459 (2025).
[72] O. Payen, S. Top, A. Vessières, E. Brulé, A. Lauzier, M.-A. Plamont, M. J. McGlinchey, H. Müller-Bunz, G. Jaouen, Synthesis and biological activity of ferrocenyl derivatives of the non-steroidal antiandrogens flutamide and bicalutamide, J. Organomet. Chem. 696 (2011) 1049–1056.
[73] A. Rashid, M. Perveen, R.A. Khera, K. Asif, I. Munir, L. Noreen, S. Nazir, J. Iqbal, A DFT study of graphitic carbon nitride as drug delivery carrier for flutamide (anticancer drug), Journal of Computational Biophysics and Chemistry 20 (2021) 347–358.
[74] Y. Yong, X. Su, Y. Kuang, X. Li, Z. Lu, B40 and M@ B40 (MLi and Ba) fullerenes as potential molecular sensors for acetone detection: a first-principles study, J. Mol. Liq. 264 (2018) 1–8.
[75] S.S. Li, Semiconductor Physical Electronics, Springer Science & Business Media, 2012.
[76] A.A. Peyghan, H. Soleymanabadi, Computational study on ammonia adsorption on the X 12 Y 12 nano-clusters (X= B, Al and Y= N, P), Curr. Sci. (2015) 1910–1914.
[77] I. Baikie, S. Mackenzie, P. Estrup, J. Meyer, Noise and the kelvin method, Rev. Sci. Instrum. 62 (1991) 1326–1332.
[78] O. Richardson, Electron emission from metals as a function of temperature, Phys. Rev. 23 (1924) 153.
[79] A. Patla, J. Pal, R. Subramanian, Theoretical investigations on the nature of interactions in ions (Li+, Na+, Be2+, Mg2+)-water clusters in the gas phase, Mol. Phys. 123 (2025) e2372454.
[80] M. Ziati, N. Bekkioui, H. Ez-Zahraouy, Ruddlesden-popper compound Sr2TiO4 doped with chalcogens for optoelectronic applications: insights from first-principle calculations, Chem. Phys. 548 (2021) 111221.
[81] P. Niknam, S. Jamehbozorgi, M. Rezvani, V. Izadkhah, Understanding delivery and adsorption of Flutamide drug with ZnONS based on: dispersion-corrected DFT calculations and MD simulations, Physica E 135 (2022) 114937.
[82] Z. Bagherzadeh, S. Hosseini, M. Esrafili Dizaji, A DFT study of pure and M-encapsulated (M=Na and K) B40 fullerenes as potential sensors for the flutamide drug, J. Mol. Graph. Model. 140 (2025) 109084.
[83] V. Nagarajan, R. Chandiramouli, Flutamide drug interaction studies on graphdiyne nanotube – a first-principles study, Computational and Theoretical Chemistry 1167 (2019) 112590.
[84] M. Barzan Talab, H. Hasan Muttashar, J. Faraj, S.A.H. Abdullaha, S.K. Hachim, M. Adel, M.M. Kadhim, A. Mahdi Rheima, Inspection the potential of B3O3 monolayer as a carrier for flutamide anticancer delivery system, Computational and Theoretical Chemistry 1217 (2022) 113886.
[85] J. Beheshtian, A.A. Peyghan, Z. Bagheri, Detection of phosgene by Sc-doped BN nanotubes: a DFT study, Sens. Actuators B 171 (2012) 846–852.
[86] N.T. Si, N.T.A. Nhung, T.Q. Bui, M.T. Nguyen, P.V. Nhat, Gold nanoclusters as prospective carriers and detectors of pramipexole, RSC Adv. 11 (2021) 16619–16632.
[87] R. Bagheri, M. Babazadeh, E. Vessally, M. Eshaghi, A. Bekhradnia, Si-doped phagraphene as a drug carrier for adrucil anti-cancer drug: DFT studies, Inorganic Chemistry Communications 90 (2018) 8–14.